R. B. Sheldon
The University of Alabama in Huntsville

T. A. Fritz
Boston University

On the Outer Radiation Belt Electron Source

Short title: ON THE ORBE SOURCE

Abstract. Outer radiation belt electrons (ORBE) at 0.1 - 10 MeV are a major hazard for geosynchronous and high altitude Earth orbiting spacecraft as well as human spaceflight. Yet despite 40 years of study, the inherent variability of these electrons make their prediction so difficult that space assets are protected by *in situ* monitors followed in real time such as those at NOAA's SEC. Although electrons are ubiquitous in neutral plasmas, electrons of this energy and density are found neither in the Earth's ionosphere nor in the Solar Wind, suggesting that these electrons gain their energy locally. Compounding the problem, is the poor correlation of solar wind energy with measured fluxes of these electrons. The fundamental problem appears to be identifying the local source of these relativistic electrons. We argue for a highly non-linear, rapid stochastic acceleration process occurring in the Earth's cusps. Only a cusp source satisfies all the observational constraints. This paper concerns itself with the evidence that ORBE are accelerated in the cusp, in a second paper, we present the physics of the quadrupolar cusp trap itself.

Introduction

The origin of the MeV electrons in the Earth's "outer radiation belt" (ORBE) has been mysterious since their discovery 40 years ago by Van Allen ([*Allen et al.*(1959); *McIlwain*(1996); *Baker et al.*(1997)]). Despite their understandably deletrious effects on space electronics, neither military nor civilian spacecraft operators are able to predict their sudden enhancements, and must rely on passive shielding and *in situ* monitors of these hazardous particles. Statistical models are valuable for *post mortems*, but are too imprecise for real-time prevention. There is still debate on whether real-time prevention is cost-effective, but the debate is clouded by the poor success rate of present predictors. By analogy to the weather bureau, preventive measures have become much more common as predictions improved. That is, we have a 40-year database on the climate of space, but have very little ability to predict the weather.

Predictors

Weak statistical links or neural net "black boxes" are the only predictors we have found in the $\sim$40 years since the ORBE discovery by Van Allen [*Allen et al.*(1959),], for if anything better were found, it would be used at NOAA's SEC. The one predictor that the SEC uses, the neural net predictor of [*Koons and Gorney*(1991),] was based on the daily sum of the previous 10 days of Kp, where the 1-day resolution was dictated by the quality of the data. Although this predictor can account for 70% of the geometric variation (variances in the logarithm) in the daily averaged, E>3 MeV integral energy electron channel from GOES geosynchronous satellites, the predictions work best at low activity level and fail rather dramatically in predicting the onset of high electron fluences (see Fig. 1). Yet this weak correlation was better than Dst or AE, which produced even smaller correlations. The one exception is the solar wind velocity correlation, V_{sw}, [*Blake et al.*(1997),], which has remained unexplained. Nor is there any explanation why Kp should work at all. What has been lacking are physical models that can direct the statistical investigation into fruitful correlations that might create better predictors of MeV electron enhancements.

Sources

Where are these electrons and why is their origin a mystery? These MeV electrons are trapped in the Earth's dipole field, at radial distances from $\sim$ 3–7 Re at the equator, forming the outer radiation belt [*Allen et al.*(1959),]. The fluxes show extreme variability, including rapid, adiabatic effects and non-adiabatic injections on the scale of hours or days, followed by a decay on a timescale of days to weeks [*McIlwain*(1996),]. A typical MeV enhancement occurs $\sim$24 hours after the beginning of a "stormy" period, and takes 0.5–2 days to reach its maximum which almost always occurs at 6.6 Re before 4.0 Re (personal communication, G. Ginet, 1997). As the Earth's dipole field weakens at larger distances, the fluctuations of the field caused by solar wind disturbances become increasingly important, so that the radial transport rate is faster than one Re per day at distances beyond 6 Re [*Schulz and Lanzerotti*(1974),]. There is even some evidence from electric field measurements that during disturbed times, this diffusive transport time can be as short as an Re per hour (personal communication, J. Wygant, 1997). And beyond 8 Re, the dipole field is so distorted that it cannot trap the electrons at all, that is, they do not possess all three adiabatic invariants of the motion and therefore are at best "pseudo-trapped" [*Roederer*(1970),].

Generally it is the third invariant that is violated most easily, meaning that the electrons cannot drift 360° around the Earth without encountering the magnetopause and becoming lost. Thus the source of these $\sim$1 day rising enhancement of MeV electrons might be argued to be in the trapping region itself, for otherwise it would appear to be a transient in the outer regions, having a lifetime of several tens of minutes, the time it takes for electrons to drift around the Earth. Yet up until POLAR, extensive searches in the trapping region have shown no acceleration region or population (observable by a peak in phase space density) that can be the source of the outer zone electrons (e.g., a "Nishida recirculation" type mechanism [*Nishida*(1976), *Paulikas and Blake*(1979), *Ingraham et al.*(1996),]).

Recent work using the high spectral resolution MeV electron spectrometer on POLAR, CEPPAD/HIST, have confirmed what other data sets have been telling us, that during quiet times, the phase space density at constant magnetic moment uniformly rises toward higher L-shells, away from the Earth [*Selesnick and Blake*(1997),]. (This is always true for quiet periods, but strictly true only for E$<$1MeV electrons during stormy periods. Selesnick in his most recent work with improved instrument calibration functions, [private communication, 1999] states that the data are most consistent with an external source. Since the existence of external source is undisputed, we refer to this source alone.) Furthermore, since the diffusive radial transport rate for these electrons during storms is quite rapid, this suggests that the source is external to the trapping region, but populates the ORBE rapidly during a storm. However, the solar wind (at infinite L-shell) has a lower phase space density than the magnetosphere whether we compare at constant energy or constant magnetic moment [*Li et al.*(1997),] and cannot be the putative source. Thus until recently we could only say that the mysterious source of these electrons lies at $7<L<\infty$.

Accelerators

This is troubling, because these high L-shells hold pseudo-trapped populations and should have lower, not higher, phase space densities than the trapped population. One solution might be to put a source within the pseudo-trapping region, which would neccessitate a rapid acceleration mechanism that could accelerate in less than a drift period (e.g., the 1991 "shock acceleration" event [*Li et al.*(1993),]), yet remain for many hours while filling the radiation belts. That is, can we replace the mysterious source with a possibly less mysterious *in situ* accelerator that has the characteristics observed in ORBE enhancements? This has been an area of active work, with suggestions that resonant wave acceleration ([*Elkington et al.*(1999)]), lightning discharges [*ehtinen et al.*(2000)]), or substorm inductive acceleration ([*Kim et al.*(2000); *Ingraham et al.*(1999)]) might be such an accelerator mechanism. However, no internal mechanism has yet been found that satisfies the observational constraints outlined below.

The Puzzle

Thus we find that ORBE enhancements remain a puzzle, with weak correlations to Kp, stronger correlations with V_{sw}, yet without an identifiable source or acceleration mechanism. However, the wise investment in GGS given us two new observations that have provided two important clues: high spectral and spatial resolution of ORBE enhancements, and continuous, high time resolution V_{sw}. With POLAR we can produce accurate radial profiles and spectral resolution to "fingerprint" the acceleration mechanism, whereas WIND (and now ACE) can deliver the high time-resolution, continuous solar wind needed to catch ORBE enhancements “in the act”.

Observational Constraints

There are several basic observational constraints that any predictive model of ORBE enhancements must address:

- 1) the radial gradient rising outward during quiet periods and flattening during storms;
- 2) the pitch-angle gradient flattening during quiet times and peaking at 90° during storms;
- 3) the 0.5-2 day time delay in the rise time of ORBE when compared to Dst or Kp rise times;
- 4) the constant spectral increase of MeV electrons below some threshold energy;
- 5) the better correlation with Kp than with Dst or AE;
- 6) the fastest correlation with noon local time; and,
- 7) the (sometimes) excellent correlation with V_{sw} or ΔV_{sw}, (and not with B_z, E_y, N_i, or $N_i V_{sw}^2$).

Transport

The first observation, which could not be argued convincingly until POLAR, though hints were available from low altitude satellites such as SAMPEX, argues that transport is occurring from the outside in. We include the pitch-angle gradient, because it is consistent with radial diffusion, peaking at 90° due to the betatron acceleration of radial transport [*Schulz and Lanzerotti*(1974),]. When transport is slow (quiet periods) the pitch-angle gradient is erased by scattering processes. This is supported by UARS measurements of MeV electron injections at low altitude, corresponding to small pitchangles, which show a time delay with respect to the equator that is well modelled by pitchangle diffusion [*Schulz et al.*(1999),]. This implies that the injection *cannot* be isotropic in pitchangle, or otherwise the low altitude observations would be simultaneous. Thus we have two choices, either the acceleration is primarily at 90°, or the acceleration occurs at large radial distances and is transported radially. When combined with the radial gradient, the second option appears most likely.

The theory of radial transport was well developed from the 1960's, where magnetic and electric impulses were shown to account for the radial diffusion and transport of radiation belt particles. This is consistent with smaller radial gradients during times of enhanced diffusive transport, and give transport rates well in excess of 1 Re/day. Thus one can show that field fluctuations measured during a magnetic storm give transport times for ORBE is on the time scale of hours (J. Wygant, 1997, private communication).

Time Delay

Thus the typical 48 hour or atypical 12 hour rise time for ORBE, cannot be attributed to purely transport delays from some external source, since transport times during storms can be as small as an hour, rather one must assume that the source itself has a similar built-in time delay. One could imagine that a solar proton event or interplanetary conditions might lead to a slow increase in ORBE, but no such extraterrestrial source has been linked to ORBE enhancements. Similar objections can be raised for *in situ* accelerators, for if the source were a nearly instantaneous injection such as occurred during the 1991 storm, it would not have the requisite 2-day time delay. This could be said for most 1st order, or single-step acceleration mechanisms such shock acceleration, reconnection electric field acceleration, inductive betatron acceleration, Fermi acceleration and so forth, they all accelerate too quickly.

This leads us to the possibility that an electron could perhaps take many small steps that prolong the acceleration process and incrementally provide the energy, say, from a series of several intense substorms (e.g, [*Ingraham et al.*(1999); *Kim et al.*(2000)]). Then time between these acceleration events would allow transport and diffusion, so that some particles would get accelerated many times, others only once. Thus this random acceleration would appear to us to be a diffusion in energy space, or a 2nd order, stochastic acceleration. The two basic requirements on any stochastic acceleration are a sufficiently energized "seed" population to start the process, and a sufficiently "trapped" population that will undergo multiple acceleration steps with some probability.

Spectral fingerprints

If the time delay is due to a slow, stochastic acceleration process, we should see the tell-tale characteristic spectral signatures of the mechanism. Since a diffusion in energy space approximates this random energization, the higher energies should appear later than the lower energies. Furthermore, the "energy slope", or spectral index (if it can be approximated by a power law), moves toward higher energy just as a temperature gradient in a copper bar moves as the heat diffuses outward. Note that under the assumption of a constant initial spectral index, a power law slope, the outcome of stochastic acceleration does not change the index, it remains a power law but now at higher amplitude. Contrast this with single step processes, (e.g., a DC electric field acceleration would harden the spectrum up to a fixed energy) which all impose a different characteristic signature on the energy spectrum. What do the data show?

When we examine the LANL geosynchronous satellites, we find that spectra taken before and after an ORBE enhancement often have identical spectral indices with merely enhanced fluxes, exactly as predicted by a stochastic process (private communication, J. Freeman98). However, we must be clear that the amplitude change cannot extrapolate to infinite energy, since the highest energies take the longest time to accelerate, longer, perhaps, than the temporal extent of the storm. Thus if stochastic processes indeed energize the spectra, there must exist some threshold energy, above which the spectra remain unchanged. Closer examination of the higher spectral resolution POLAR/HIST data show exactly this characteristic, a sharp bend in the spectral index at the higher energies, $E > 3$MeV. This break is consistent with the stochastic acceleration time becoming longer than the duration of the event. Furthermore, during the fastest ORBE enhancement of the last 3 years, January 10, 1997, the spectral index displayed a lower than usual break in the spectral index, at E $<$ 2 MeV.

Kp/AE/Dst

If the acceleration mechanism is stochastic, then this probably indicates why Dst is not a good predictor of the ORBE increases: Dst is primarily a single-step process, a rapid change followed by a gradual return. ([*Reeves*(1998)] shows a surpising joint occurrence probability between Dst and ORBE, which [*Sheldon*(2000)] argues is not causal.) Therefore the absolute level of Dst (other than the initial adiabatic decrease of the ORBE occurring during main phase) gives no indication of the multi-step strength of the ORBE enhancement. So it is not surprising that Kp is a better indicator than Dst. More significantly we find that Kp is better than AE, that disturbances at midlatitude are a better indicator of ORBE increases than disturbances at high latitude which map to the tail. This brings into question any acceleration mechanism that involves tail disturbances, which would presumeably have better correlation with AE than Kp.

LT

Work with AZORA data at low altitude show that fluctuations in MeV electrons are best correlated in the noon quadrant [*Fung and Tan*(1998),] especially at very short time scales. If the acceleration mechanism produced *any* small pitchangle particles, one would expect a sharp spike at low altitude during the injection followed by a gradual rise as pitch angle diffusion flattened the bulk of the distribution. Thus Fung's analysis is consistent with a dayside injection, and inconsistent with a substorm or tail source. A careful analysis of the January 11, 1997 event showed that the noon quadrant also showed the first arrival of the 1000-fold increase of ORBE electrons (private communication, G. Reeves 1997).

V_{sw}

The best clue is the high correlation (R=70!) of solar wind speed with ORBE enhancements. Converting V_{sw} to $E_y = V_{sw} \times B$ ruins the correlation, as does the conversion to $p = N_i V_{sw}^2$. That is, when we convert the solar wind velocity to either mechanical or electrical energy, we find the correlation is worse. Yet how else are we to couple the energy of the solar wind to the ORBE?

The message in this data is that the ORBE is not directly driven, or else there should be a better correlation with the driving energy. Or mathematically, we might say that the response is non-linear. Using our discussion of stochastic acceleration as a guide, we might argue that, say, reconnection E_y is the energy driver, but thermalized V_{sw} is the seed-population energy. Thus higher velocity may lead to both a higher energy driver and a higher temperature seed population in a way that gives more correlation with velocity than with energy alone.

Solar Wind Statistics

We have correlated the GOES E1 channel (electrons with E>2MeV) with solar wind conditions as monitored by IMP-8. Since IMP-8 Omni data is available at 1 hour resolution, we have rebinned our GOES data into 1 hour bins as well. As observed by Paulilakis and Blake, the most significant correlation is with V_{sw} and for southward B_z. The data also show the highest correlations between 24-48 hour time lags, as previously noted.

What is perhaps not expected is the sometimes better correlation of MeV ions with B_z northward. This suggests that there is a non-electrical aspect to the stochastic acceleration process, which is in some sense, independent of E_y. In addition, the subset of the fastest 1/3 V_x possess nearly all the positive correlations, with the slowest 1/3 showing a negative correlation. Clearly a non-linear effect is coupling solar wind velocity into ORBE.

Model Constraints

With the above discussion, we have motivated a stochastic acceleration mechanism for ORBE enhancements occurring somewhere at large distances, L>7 Re from the Earth though probably not down tail. This mechanism must take both mechanical and electrical energy from the solar wind in a non-linear fashion. The acceleration times must be on the order of hours to days. Based on these well-accepted observational constraints, we outline a model that has 3 parts:

$$[\mathrm{SOLARWIND}, V_{sw}] \longrightarrow [\mathrm{StochasticAccelerator}] \longrightarrow [\mathrm{ORBE}] \tag{1}$$

where the box marked “ORBE” would follow the lead of Temerin (M. Temerin, GGS workshop, 1997) and Selesnick (R. Selesnick, private communication, 1998) using a time-dependent radial diffusion model to bring the ORBE in from a time-variable boundary condition around L=7 Re. These models have already been shown to qualitatively describe the shape and temporal evolution of ORBE enhancements, if they are given an appropriate enhanced boundary condition. Thus the key to achieving a successful model prediction lies in the middle box, the time variation of the outer boundary condition.

Input Constraints

The input constraints are provided by the statistical data we discussed above. The accelerator must be correlated with V_{sw}, with Kp, and with the ancillary findings of B_z northward, as well as high dV_{sw}/dt. As we pursue these statistics carefully, we also expect to find a SM dipole tilt dependence, and a time lag as described by [*Fung and Tan*(1998),] who analyzed low altitude EXOS-B electron data.

Rather than piping all these constraints into a multi-layer neural net and hoping for the best, we learn from Chen's work on neural net predictors of magnetic storms ([*Chen et al.*(1997)]), that neural nets work best when constrained by physical laws. Thus we attempt to write a differential equation expressing the dependence of the acceleration region to each of these effects, weighting each input with a coupling constant that will be determined from fitting to the data. For example, if V_{sw} is the "seed" population for a stochastic acceleration, then the rapidity with which electrons reach a certain energy is given by the Fermi mechanism equation [*Fermi*(1949),]:

$$T = T_0 e^{\alpha t} \tag{2}$$

where $T_0 = 0.5 m V_{sw}^2$ is the initial "seed" energy, α is the (energy dependent) energy diffusion rate, and t is the time.

Likewise, if we say that the time rate of change of ORBE in some energy bounded subset is proportional to their density, N, divided by some characteristic loss time, τ,

$$dN/dt = N_0/\tau \longrightarrow N(>t) = N_0 e^{-t/\tau} \tag{3}$$

Which when combined with equation 2, gives us the familiar power law tail,

$$N(>E) = N_0 \left(\frac{T_0}{T}\right)^{1/\alpha\tau} \tag{4}$$

This theory predicts that the production of MeV electrons is exponentially related to the energy of the seed population that begins the process. This is an important constraint that goes into the coupled differential equations describing the "efficiency" of the stochastic acceleration box. Similarly there are arguments for the trapping time τ that depend on IMF B_z, dipole tilt, and solar wind pressure, among others. However, there may be more than one physical model for how the trapping time depends on, say, solar wind pressure. As we discuss later, direct observations by POLAR of the trapping region will be crucial in narrowing down the possibilities.

Output Constraints

Just as solar wind monitors provide input constraints on the stochastic accelerator, so also measurements of the electrons resulting from this accelerator also put stringent constraints on it. Note that the spectral index depends crucially on the trapping time, τ. Thus for times shorter than this, $t < \tau$, we expect a power law, but for times longer, $t > \tau$, we expect no energy change at all. This "break" in the power law towards a more negative index (softer spectrum) then specifies the trapping time of the accelerator. Thus the high spectral resolution POLAR/HIST instrument is crucial toward ascertaining the trapping time and energy diffusion rate of the acceleration region.

***In Situ* Constraints**

We want to emphasize that the above model can be developed quite completely *without ever observing the trapping region*. Such models have been developed for Jupiter, for example. Clearly, however, direct observations of the trapping region will advance the model more rapidly than incremental iterative fits. For example, if the trapping time is time variable, as gross comparisons of the spectral indices of ORBE enhancements suggest, we must apply additional constraints to the model beyond what we can learn from simple spectra. Fortunately, POLAR is in a high latitude orbit that precesses around the magnetosphere in 6 months and therefore made a complete sampling (at high latitude) the $3<\mathrm{L}<\infty$ region. The discovery of trapped, energetic electrons at L$\sim$12 on the dayside was serendipitous, providing simultaneously a trapped population of electrons and a measurement of the energy drivers.

Thus we are confident that the *in situ* constraints, combined with the new high-resolution data sets are sufficient to construct an empirical model of α, the energy diffusion rate, and τ, the trapping time, so as to model a time-dependent accelerator for the source boundary of ORBE. Since these observations have only recently been published [*Chen et al.*(1997), *Chen et al.*(1998), *Sheldon et al.*(1998),], we review them briefly.

Observations of the Trap

We have observed energetic electrons (30<E<2000 keV) trapped in the outer cusp, Figure 3, a region which can be unambiguously identified by the well-instrumented POLAR spacecraft.

The Outer Cusp

POLAR is in a 2 × 9 Re orbit that on October 14, 1996, passed through the nominal outer cusp before traversing the radiation belts. The outer cusp is defined to be a region inside and adjacent to the magnetopause (7–10 Re), with noticeably reduced magnetic field strengths, having broadband electromagnetic wave power, and generally within some radial distance (2–3 Re) of the topological minimum B point. We do not define the outer cusp with respect to a particle population for the same reason that the plasmasphere, radiation belts, and ring current define overlapping regions in the dipole magnetosphere. We observe a trapped electron population in the outer cusp on this orbit, and more generally during the two seasons per year when the POLAR orbit precesses through this region (with over 90% probability of observation when orbits are favorable). Data from TIMAS and HYDRA on this day show that the magnetopause was first crossed at 0100, at which time EFI showed an abrupt increase in broadband noise. HYDRA showed brief bursts of sheath electrons between 0100–0230 that appeared to be anti-correlated with IES and HIST trapped electrons. These short magnetopause crossings ceased by 0230 along with most of the EFI wave power.

Phase Space Densities

In Figure 3 we plot time/energy/roll-angle spectrograms of phase space density from the CEPPAD/HIST and CEPPAD/IES electron instrument [*Blake et al.*(1995), *Contos*(1997),] on the POLAR spacecraft. The vertical stripes in the upper panels are an instrument artifact caused by mode switching of the HIST telescope. Successive panels are logarithmically spaced in energy where each panel displays the roll modulation (pitch angle) of the particles. The inset plots the average count rate from 0-20 cts/s in 16 pitchangle sectors, summed between 0100 and 0330 UT showing that the fluxes are clearly peaked around 90°. The color scale displays the logarithm of f (s^3/km^6) from 0.00001 (purple) to 100 (red). The left half of the plot shows 30–1000 keV electrons with trapped pitch angle distributions located in the outer cusp at L>10. The right half of the plot is an outer radiation belt traversal. Comparing the radiation belt and cusp loss cones, we see that the cusp's is much wider, which is characteristic of a "leaky magnetic bottle". It also appears that the wide loss cone of the cusp is filled at a very low, isotropic level. Comparing the phase space densities at equal magnetic moment (black dots at 7.4 keV/nT), reveals that the outer cusp has equal or higher densities than the outer radiation belts, allowing the possibility of inward diffusion at constant first invariant. Note that the radiation belt pass is at high latitude so that the electron flux would map into the wide loss cones of the outer cusp, suggesting that the second invariant is not conserved if the cusp is the source of these electrons. These observations are very suggestive, and led us to simulate these particles to understand these signatures.

Locally Trapped

Now this trapped cusp population is highly unusual because, classically speaking, the cusp cannot trap particles at all [*Roederer*(1970),], it is not an "excluded region" in the Störmer theory of an idealized dipole [*Störmer*(1911), *Rossi and Olbert*(1970),]. However, the interaction of a magnetic dipole with the solar wind modifies the topology in a fundamental way that has not been adequately considered in the theory of trapped particles; rather than a dipole, the cusp appears to be quadrupolar. We demonstrate the existence of this particle trap using the somewhat extreme geomagnetic conditions of a nearly minimum latitude cusp and a high speed solar wind, producing a nominal standoff distance of $\sim$11 Re.

When we trace particles through this region we find trapping to occur when the electrons mirror around the local minimum of the field line found at the center of the cusp. The orbits take the shape of a lily, with a locally outward magnetic gradient instead of the typical inward gradient so that the particles drift 360° around the cusp in an opposite sense to the trapped radiation belt particles. Our results show that 5–5000 keV electrons can be trapped in the cusp of a T96 magnetosphere for $\tau > 300$ seconds, though admittedly without an electric field (see Figure 4). Examination of particle trajectories in this region shows that although they lack a dipolar second and third invariant, since they never cross the dipole magnetic equator, we can find an analogous second and third "cusp" invariants of the motion if we define the "cusp equator" to be the surface of minimum $|B|$ along a field line that approaches the cusp. Thus we can uniquely identify these invariants in analogy to B-L space by their pitch angle and $|B|$ at the crossing of the cusp equator. In Figure 4 one can see three nested "cusp-shells" analogous to

L-shells of the dipole. The limiting 2nd invariant of these trapped orbits occurs when the mirror point $|B_m|$ approaches the dayside equatorial field strength, at which point the electrons join the dipolar pseudo-trapped population and ∇B drift away from the cusp. From the pitch angle distribution, this value appears to be $\alpha_0 \sim 60°$. The limiting 3rd invariant is the maximum value of $|B|$ for which the "cusp equator" is still defined over a closed, 360° loop.

Locally Accelerated

Are these trapped particles accelerated *in situ*? Because the phase space density is higher in the trap than either in the solar wind (shocked magnetosheath) or in the neighboring dipole trap, the conclusion that acceleration is local appears inescapable. In fact, the $|B|$ minima seen at the cusp are so low, a 90° particle at this location cannot leave the trap without destroying its 2nd invariant. Now the faint background level inside the wide cusp loss cones could be understood as dipole-trapped particles that have drifted into the bifurcated dayside minima in their drift orbit around the earth, but the peak at 90° can only be locally trapped, cusp particles. One might invoke multistep processes that violate entropy, but simple physics dictates that the higher phase space densities observed in this trap are the result of a local acceleration process.

Cusp Acceleration

How would this cusp trap accelerate electrons? First we might ask how acceleration occurs in the dipole trap. Generally speaking, the dipole trap accelerates particles when one or more of the adiabatic invariants of the motion are violated by disturbances that have shorter timescales than the associated period of the motion. For example, random magnetosphere compressions from the solar wind with a typical 8-minute period have no effect on the first or second adiabatic invariants, but the violate the third invariant, causing radial diffusion and the energization of the ring current [*Sheldon and Hamilton*(1993),].

Energy Diffusion Rate, α

The cusp, however, has an important advantage over the dipole trap, in that the three periods of the motion lie much closer to each other. For example, when the magnetic field becomes very weak, the gyration becomes very long (and Larmor radius very large) so that inhomogeneities in the field violate the first invariant and lead to energy diffusion. As [*Delcourt et al.*(1992),] has shown, the magnetic moment of these trapped electrons need not be conserved as they pass near the minimum B-field point. In more mathematical terms, one says that disturbances that resonate with the frequency of one of the periods of the motion violate that invariant most efficiently, leading to a diffusion of that invariant [*Schulz and Lanzerotti*(1974),]. The particular invariant invoked is not crucial in principle, because there are mechanisms to produce energy diffusion from the violation of each.

In addition, if two resonances overlap, then the phase space density changes even more chaotically, such that stochastic acceleration is most effective when the frequencies associated with each adiabatic invariant are nearly commensurate. That is, near the minimum field point, the time scales of the adiabatic invariants converge, (see Fig. 4) meaning that the level of turbulence, $\Delta B/B$ needed to initiate chaotic trajectories in phase space (producing an “Arnol’d web” and rapid chaotic acceleration [*Arnol’d*(1964),] is much lower. Hence the cusp is inherently more energy diffusive than the dipole trap.

Yet a third factor makes the cusp a more effective accelerator than the dipole: the observation of cusp diamagnetic cavities [*Chen et al.*(1997),]. In hindsight, the weak field region of the central cusp adjacent to the high plasma densities of the sheath might have led theorists to predict such cavities. The important point in this discussion, is that such cavities have large magnetic fluctuations, the largest in the magnetosphere, simultaneous with low magnetic field strengths. These conditions are optimal for coupling energy from the fluctuations into a chaotically broadened resonance of the trapped electrons, thereby increasing by an order of magnitude, the fluctuation power available.

Trapping time, τ

Despite the evidence of sufficient power to drive a stochastic acceleration process, we must also ask whether there is sufficient trapping time to produce MeV electrons from a KeV source population. Ideally we would tag some cusp electrons and observe their trapping times, but since all electrons appear identical, we turn to solar wind ions as a “tracer” of particle trapping. On May 29, 1996, the POLAR/CAMMICE instrument observed solar wind O^{6+} ions deep in the cusp, nearly 2 hours after a brief interlude of B_z southward in the midst of a strongly Bz northward solar wind stream

[*Grande et al.*(1997),]. We then adjust the timescale from a 500 keV oxygen ion to a 5 keV electron and conclude that electrons are trapped in the cusp for at least 10 minutes. Using the Bohm diffusion rate purely as an upper limit on stochastic acceleration (since the gyroperiod is the shortest of the resonant periods we might imagine using), we calculate that this same 5 keV electron will reach 1 MeV energies in the presence of a resonant 10 mV/m cusp electric field (a typical cusp AC field as observed by POLAR/EFI) in about 8 seconds. Scaling the period to a bounce or a drift resonance near the center of the cusp gives us 80 or 800 seconds, both near the 10 minute estimated trapping time. Thus we appear to have enough time for stochastic acceleration to operate on this trapped population.

Seed Population, T_0

Stochastic acceleration is dependent upon a minimum energy "seed population" that can diffuse in energy space. Since in these processes, the energy gain is often proportional to the initial energy, a seed population with lower energy will take considerably longer to accelerate, perhaps longer than the trapping time. Since the trapping time can be a strong function of energy as well, this produces a sharp cutoff in the lowest energy that can be accelerated by the mechanism.

This minimum energy seed population may not always be available in the shocked magnetosheath plasma. That is, when electric fields are superposed on the cusp trap there exists a minimum energy electron above which ∇B drifts dominate over E×B and permit trapping, in complete analogy to the dipolar plasmapause. Thus slight variations in the temperature of the seed population, or in the DC electric field of cusp could result in large variations in the density of the "seed population" and therefore in accelerator efficiency. Both of these processes are controlled by reconnection ([*Fuselier et al.*(1999)]), making IMF B_Z an important controlling factor. Finally, the nightside trapped population also overlaps the cusp as it bifurcates on its drift from the nightside ([*Shabansky*(1971)]), making substorm injections also important as a seed population. All these putative sources must be pitchangle scattered to become trapped in the cusp (with its very small $|B|$), so that the presence or absence of waves resonant with the gyrofrequency can strongly affect the seed population and accelerator efficiency.

The fluctuation power driving the acceleration mechanism may also be highly time-variable depending on reconnection rates or variations in the solar wind pressure. For example, the well-known

27-day recurrence of MeV electron enhancements has been tied to high speed solar wind streams, which are known to have higher fluctuation power as well. The only solar wind parameter better correlated to ORBE than $V_s w$, is $\Delta V_s w$ with a R=75 linear correlation factor (private communication, M. Temerin, 1997). Sorting out the importance of all these effects will require a better understanding of the cusp dynamics.

Conclusions

We have attempted to show how the ORBE source is consistent with a stochastic acceleration process occurring in the cusp, and is the only hypothesis that meets all seven observational constraints. However, we recognize that the strong non-linearities of the cusp process, preclude a linear predictive model, until the physics of cusp trapping, cusp diamagnetic cavities, and coupling to the solar wind are described in better detail. That is the task of the second paper.

Acknowledgements

We gratefully acknowlege the support of the CAMMICE team, and NASA grant NAG-5??, which supported this work.

References

Allen, J. A. Van, C. E. McIlwain, and G. H. Ludwig. Radiation observations with satellite 1958ϵ. *J. Geophys. Res.*, *64*, 271–286, 1959.

Arnol'd, V. I. *Dokl. Akad. Nauk. SSR*, *156*, 9, 1964.

Baker, D. N., X. Li, N. Turner, J. H. Allen, L. F. Bargatze, J. B. Blake, R. B. Sheldon, H. E. Spence, R. D. Belian, G. D. Reeves, S. G. Kanekal, B. Klecker, R. P. Lepping, K. Olgivie, R. A. Mewaldt, T. Onsager, H. J. Singer, and G. Rostoker. Recurrent geomagnetic storms and relativistic electron enhancements in the outer magnetosphere: Istp coordinated measurements. *J. Geophys. Res.*, *102*, 14,141–14,148, 1997.

Blake, J. B. et al. CEPPAD: Comprehensive energetic particle and pitch angle distribution experiment on POLAR. In C. T. Russell, editor, *The Global Geospace Mission*, pages 531–562. Kluwer Academic Publishers, 1995.

Blake, J. B., D. N. Baker, N. Turner, K. W. Olgivie, and R. P. Lepping. Correlation of changes in the outer-zone relativistic-electron population with upstream solar wind and magnetic field measurements. *Geophys. Res. Lett.*, *24*, 927–929, 1997.

Chen, J., T. A. Fritz, R. B. Sheldon, H. E. Spence, W. N. Spjeldvik, J. F. Fennell, and S. Livi. A new temporarily confined population in the polar cap. *Geophys. Res. Lett.*, *24*, 1447–1450, 1997.

Chen, J., T. A. Fritz, R. B. Sheldon, H. E. Spence, W. N. Spjeldvik, J. F. Fennell, S. Livi, C. Russell, and D. Gurnett. Cusp energetic particle events: Implications for a major acceleration region of the magnetosphere. *J. Geophys. Res.*, *103*, 69–78, 1998.

Contos, A. R. Complete description and characterization of the high sensitivity telescope (hist) onboard the polar satellite. Master's thesis, Boston University, Boston, MA, 1997.

Delcourt, D. C., T. E. Moore, J. A. Savaud, and C. R. Chappell. Nonadiabatic transport features in the outer cusp region. *J. Geophys. Res.*, *97*, 16,833–16,842, 1992.

ehtinen, N. G., U. S. Inan, and T. F. Bell. Trapped energetic electron curtains produced by thunderstorm driven relativistic runaway electrons. *Geophys. Res. Lett.*, *27*, 1095–1098, 2000.

Elkington, S. R., M. K. Hudson, and A. A. Chan. Acceleration of relativistic electrons via drift-resonant interaction with toroidal-mode pc-5 ulf oscillations. *Geophys. Res. Lett.*, *26*, 3273–3276, 1999.

Fermi, E. *Phys. Rev.*, *75*, 1169, 1949.

Fung, S.F. and L.C. Tan. Time correlation of low-altitude relativistic trapped electron fluxes with solar wind speeds. *Geophys. Res. Lett.*, *25*, 2361–2364, 1998.

Fuselier, S. A., M. Lockwood, T. G. Onsager, and W. K. Peterson. The source population for the cusp and cleft/llbl for southward imf. *Geophys. Res. Lett.*, *26*, 1665–1668, 1999.

Grande, M., C. H. Perry, A. Hall, J. Fennell, and B. Wilken. Survey of ring current composition during magnetic storms. *Adv. Space Res.*, *20*, 321–326, 1997.

Ingraham, J. C., T. E. Cayton, R. D. Belian, R. A. Christensen, F. Guyker, M. M. Meyer, G. D. Reeves, D. H. Brautigam, M. S. Gussenhoven, and R. M Robinson. Multi-satellite characterization of the large energetic electron flux increase at l=4–7 in the five-day period following the march 24, 1991, solar energetic particle event. In G. D. Reeves, editor, *Workshop on the Earth's Trapped Particle Environment*, pages 103–108. AIP Press, Woodbury, NY, 1996.

Ingraham, J.C., R. D. Belian, T. E. Cayton, M. M. Meier, and G. D. Reeves. March 24, 1991, geomagnetic storm: Could substorms be contributing to relativistic electron flux buildup at geosychronous altitude? *Eos Supplement*, *80*, S294, 1999.

Kim, H.-J., A. A. Chan, R. A. Wolf, and J. Birn. Can substorms produce relativistic outer belt electrons? *J. Geophys. Res.*, *105*, 7721, 2000.

Koons, H. C. and D. J. Gorney. A neural network model of the relativistic electron flux at geosynchronous orbit. *J. Geophys. Res.*, *96*, 5549–5556, 1991.

Li, X., I. Roth, M. Temerin, J. R. Wygant, M. K. Hudson, and J. B. Blake. Simulation of the prompt energization and transport of radiation belt particles during the March 24, 1991 SSC. *Geophys. Res. Lett.*, *20*, 2423–2427, 1993.

Li, Xinlin, D. N. Baker, M. Temerin, D. Larson, R. P. Lin, G. D. Reeves, M. Looper, S. G. Kanekal, and R. A. Mewaldt. Are energetic electrons in the solar wind the source of the outer radiation belt? *Geophys. Res. Lett.*, *24*, 923–926, 1997.

McIlwain, C. E. Processes acting upon outer zone electrons. In J. F. Lemaire et. al, editor, *Radiation Belts Models and Standards*, Washington DC, 1996. AGU.

Nishida, A. Outward diffusion of energetic particles from the Jovian radiation belt. *J. Geophys. Res.*, *81*, 1171, 1976.

Paulikas, G. A. and J. B. Blake. Effects of the solar wind on magnetospheric dynamics: Energetic electrons at geosynchronous orbit. In W. P. Olson, editor, *Quantitative Modelling of Magnetospheric Processes, Geophys. Monogr. Ser.*, volume 21, page 180, Washington, D.C., 1979. AGU.

Reeves, G. D. Relativistic electrons and magnetic storms: 1992-1995. *Geophys. Res. Lett.*, *25*, 1817–1820, 1998.

Roederer, J. G. *Dynamics of Geomagnetically Trapped Radiation*. Springer, New York, 1970.

Rossi, B. and S. Olbert. *Introduction to the Physics of Space*. McGraw-Hill Book Co., New York, 1970.

Schulz, M. and L. J. Lanzerotti. *Particle Diffusion in the Radiation Belts*. Springer-Verlag, New York, 1974.

Schulz, M., D. Chenette, E. Gaines, J. Hawley, R. Goldberg, and W. Pesnell. Post-storm evolution of relativistic electron pitch-angle distributions. *EOS Trans. Suppl.*, *80*(17), S306, 1999.

Selesnick, R. S. and J. B. Blake. Dynamics of the outer radiation belt. *Geophys. Res. Lett.*, *24*, 1347–1350, 1997.

Shabansky, V. P. Some processes in the magnetosphere. *Space Sci. Rev.*, *12*, 299–418, 1971.

Sheldon, R. B. and D. C. Hamilton. Ion transport and loss in the earth's quiet ring current 1. data and standard model. *J. Geophys. Res.*, *98*, 13,491–13,508, 1993.

Sheldon, R. B., H. E. Spence, J. D. Sullivan, T. A. Fritz, and Jiasheng Chen. The discovery of trapped energetic electrons in the outer cusp. *Geophys. Res. Lett.*, *25*, 1825–1828, 1998.

Sheldon, R. B. The bimodal magnetosphere and radiation belt, ring current and tail transducers. *Adv. Space Res.*, *25*, 2347–2356, 2000.

Störmer, C. Sur les trajectories des corpuscules electrises dans l'espace sous l'actions des magnetisme terrestre avec application aux auarores boréales, seconde memoire. *Arch. Sci. Phys. Nat. Ser. 4*, *32*, 117–123, 1911.

Physics Dept., UAH, Huntsville AL, 35899

Received ________________________

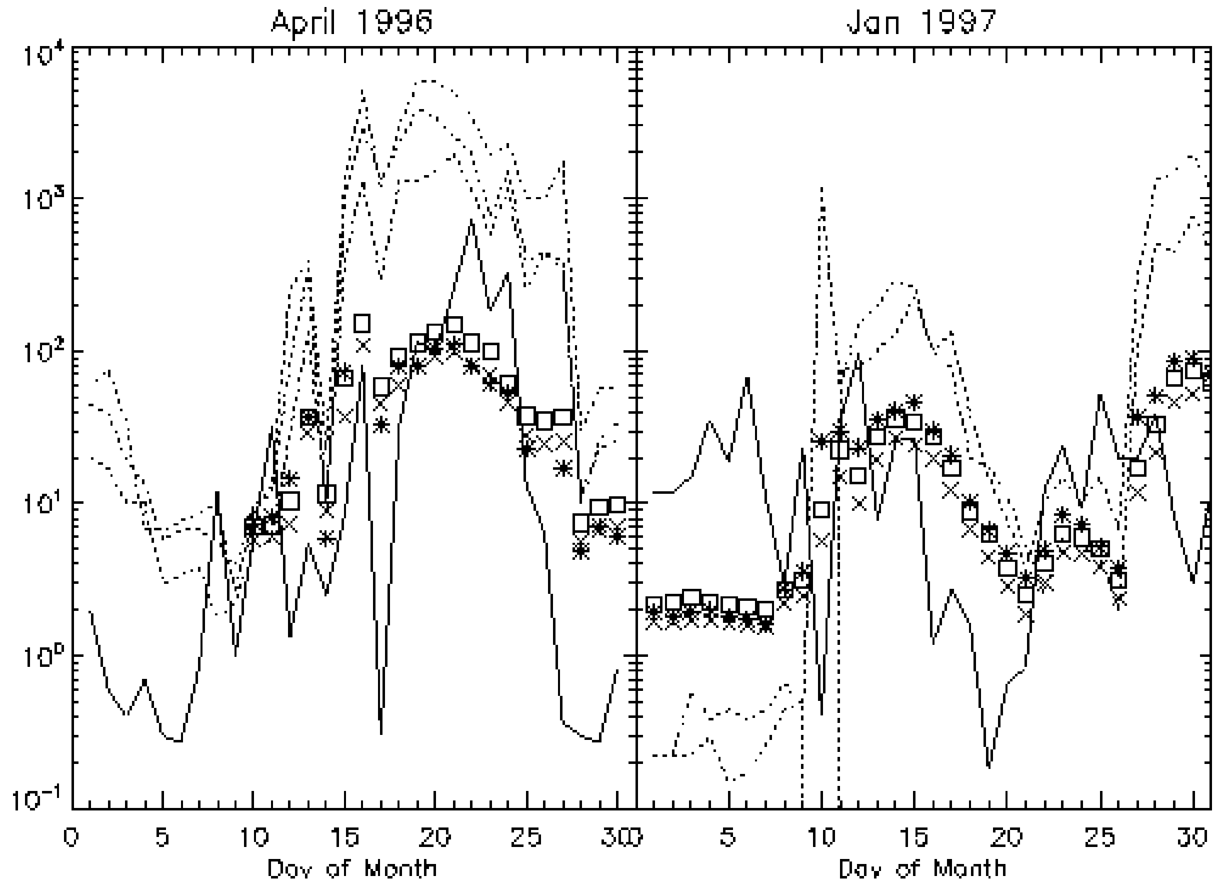

Figure 1. MeV electron enhancements where solid line is [*Koons and Gorney*(1991),]; dashed line is GOES E>3MeV; symbols are LANL 1.1-1.5 MeV electrons; all in arbitrary units.

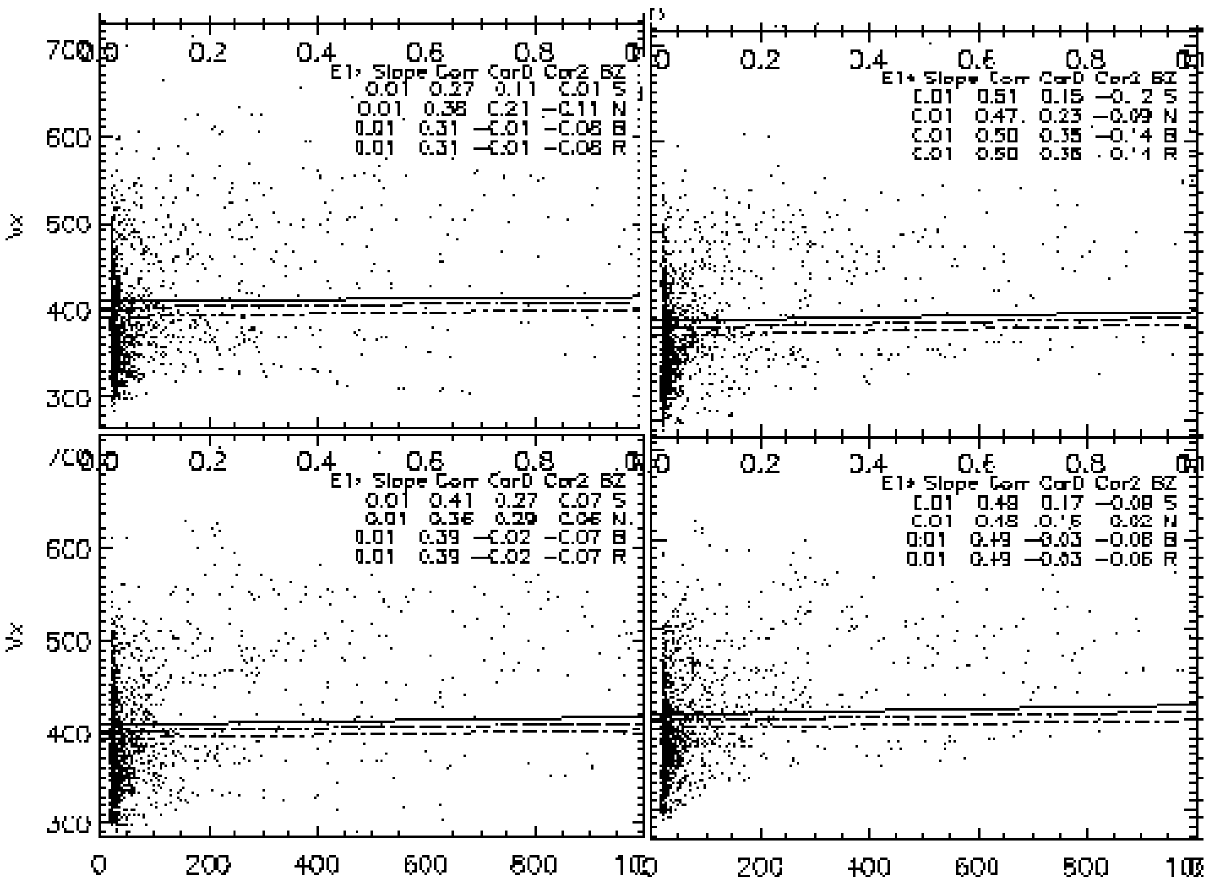

Figure 2. Scatterplot of solar wind IMP-8 V_x 1996 hourly averages correlated with GOES7 E1 energetic electrons. Upper left panel occurs at 0 time lag, lower left at 12 hour lag, upper right at 24 hour lag, and lower right at 48 hour lag. Correlation coefficients R are printed in each row for subsets of V_x sorted by southward, northward, both, and rectified signs of B_z. The first column is the slope of the fit, second column is the fit to the fastest 1/3 V_x, third column is the middle 1/3, and fourth column is the slowest 1/3 V_x.

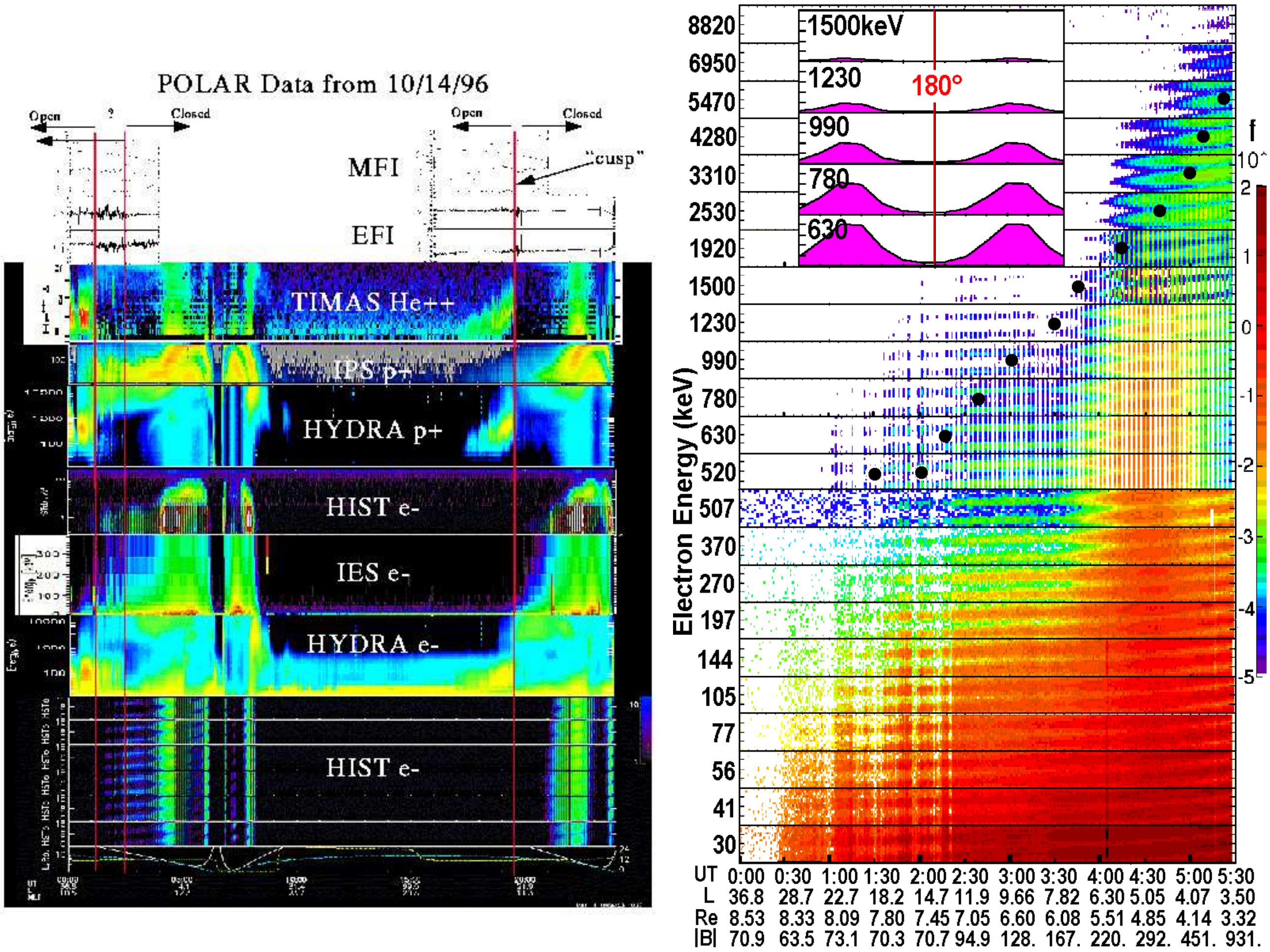

Figure 3. Left panels show POLAR overview of 14-Oct-96. Right panel zooms in on electrons from 0000-0530UT. See text for details.

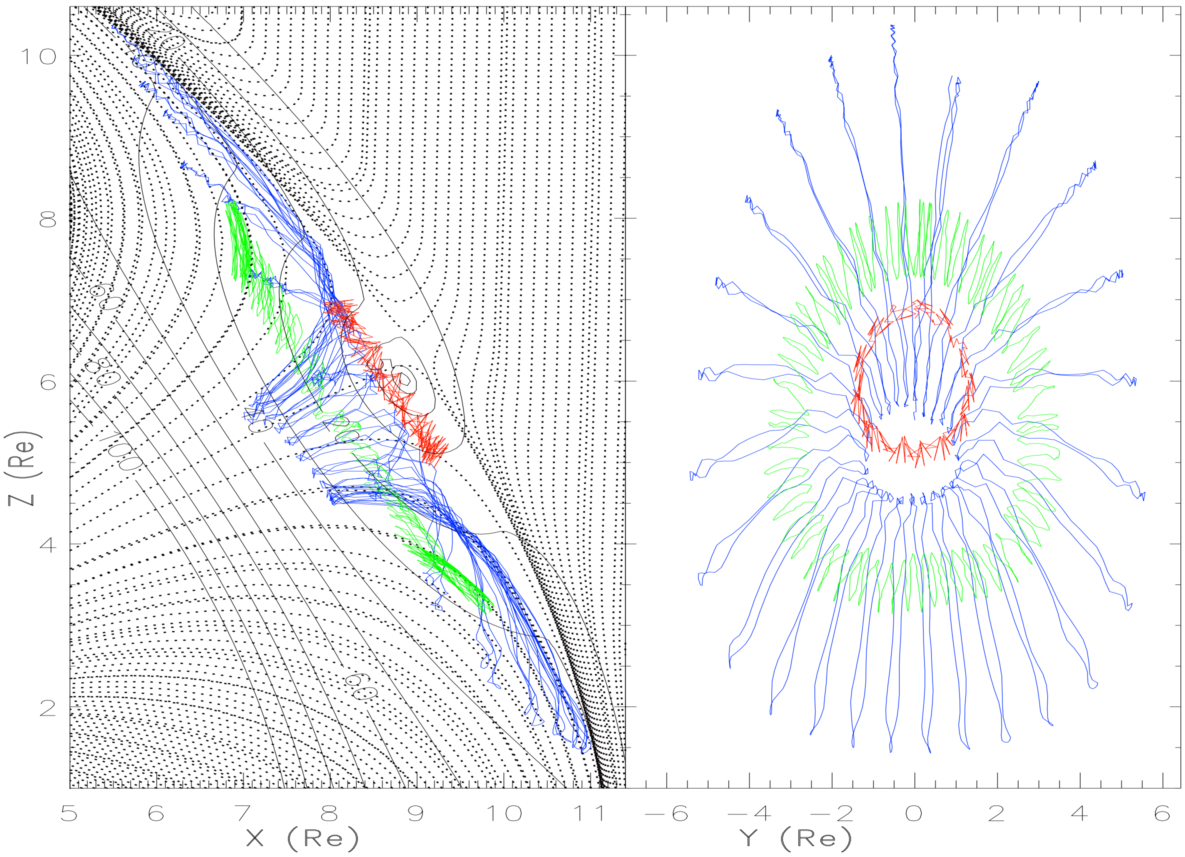

E	μ	B_0	α_0	τ_0	τ_1	τ_2
keV		nT	$\circ$	ms	s	s
1000	32.2	26.4	41	4	1.0	77
1000	30.7	21.2	35	6	1.1	67
1000	43.4	12.8	32	9	0.6	28
1000	295	6.7	88	16	0.1	1.3
95	5.4	4.8	30	7	0.2	10
5	4.5	1.1	85	40	0.4	14

Figure 4. Trajectories of trapped 1 MeV electrons in the the Earth's outer cusp, projected into the GSM X-Z and Y-Z planes. Dashed lines are field lines from the T96 magnetic field model (Dipole: June 21, 1996, 1300UT; Solar Wind: +10nT Bz, 1/cm^3, and 1000km/s V$_{SW}$). Black lines are contours of $|B|$ in nT. Green, blue and red trajectories correspond to the 1,3,4 entries of table at right.